IMAGE SEQUENCE SUPER-RESOLUTION BASED ON LEARNING USING FEATURE DESCRIPTORS

Ana Carolina Correia Rézio, William Robson Schwartz, Helio Pedrini
Institute of Computing, University of Campinas, Campinas-SP, Brazil, 13083-852

Keywords: Super-resolution, machine learning, feature descriptors, image resolution.

Abstract: There is currently a growing demand for high-resolution images and videos in several domains of knowledge, such as surveillance, remote sensing, medicine, industrial automation, microscopy, among others. High resolution images provide details that are important to tasks of analysis and visualization of data present in the images. However, due to the cost of high precision sensors and the limitations that exist for reducing the size of the image pixels in the sensor itself, high-resolution images have been acquired from super-resolution methods. This work proposes a method for super-resolving a sequence of images from the compensation residual learned by the features extracted in the residual image and the training set. The results are compared with some methods available in the literature. Quantitative and qualitative measures are used to compare the results obtained with super-resolution techniques considered in the experiments.

1 INTRODUCTION

The resolution of a digital image is directly related to its quality. This resolution refers to the level of detail of its visual representation, that is, the higher the resolution, the greater its precision to represent it in relation to the actual image (Chaudhuri, 2001a).

In many applications, an image or a sequence of images presents poor quality due to several physical limitations of the sensors, such as low spatial resolution, optical distortions, noise, and limited dynamic range (Bascle et al., 1996). In general, these degradations seriously undermine the process of image analysis. In surveillance systems, for example, images captured from low cost cameras may hinder the recognition of individuals or the identification of a vehicle license plate at a certain scene (Lin et al., 2005). In addition, a person or an object usually occupies a small region in the field of camera view, such that the portion of pixels of interest in the image is usually very small.

In several fields of knowledge, such as medicine, biology, geology, industrial automation, surveillance, remote sensing, among others, there is a great demand for high-resolution images (Chaudhuri, 2001b; Patti and Altunbasak, 2001).

Due to factors associated with cost and limitations of acquisition devices, an alternative is to increase the resolution and improve the psicovisual quality of the images by applying super-resolution techniques. Some images can suffer from a process of degradation of its quality (low resolution images) due to some factors, such as lens aberration, incorrect focus, sensor displacement during acquisition, object displacement, lack or excess of lighting (Bascle et al., 1996).

Super-resolution techniques have received much attention in recent years (Liu et al., 2008; Lucien, 1999; Lin et al., 2005; Sun et al., 2008; Baker and Kanade, 2002), whose main objective is to increase the spatial resolution of images, removing distortions in the acquisition, highlighting details, such as borders, or recovering important information from the set of images.

Super-resolution techniques can be applied to a single image, a sequence of multiple images, or videos. Super-resolution methods for a single image aim at increasing the image resolution from the enhancement of its most relevant information, without introducing blurring. Figure 1 illustrates images at low and high resolution. Super-resolution methods for multiple images seek to create an image with higher resolution from fusion information present in multiple low resolution images. Super-resolution methods for videos aim at generating a high-resolution video from low-resolution frames.

The development of techniques for increasing the sharpness of image details becomes important, since they can improve subsequent steps of data analysis and interpretation.

This paper presents a learning-based method for generating high resolution images from corresponding versions of the images at low-resolution. Unlike

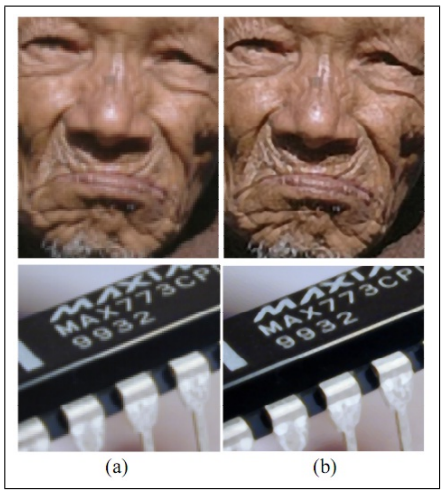

Figure 1: Examples of images (a) at low resolution and (b) at high resolution. Images extracted from (Sun et al., 2010).

the technique developed by Yu et al. (Yu et al., 2008), this work presents a methodology for super-resolution also based on locally linear embedding (LLE) and residual compensation, however, the representation of the residual is carried out by means of feature descriptors, which allows a better estimation of the super-resolved images and avoids various artifacts. Additionally, the proposed method applies a more robust technique for estimating the initial super-resolved image than that used by Yu et al. (Yu et al., 2008), called prior gradient profile (GPP) (Sun et al., 2010), which has a greater focus on edge preservation. The method is proposed for super-resolving multiple low-resolution images, instead of only a single image, on a high resolution image.

For extraction of feature descriptors, the method uses the histogram of shearlet coefficients (HSC) (Schwartz et al., 2011). The HSC is based on an accurate multi-scale analysis provided by the shearlet transform and the use of histograms for estimating the distribution of edge orientation. Experimental results show that the description of the residual using HSC provides a significant reduction of artifacts resulting from the application of super-resolution. The effectiveness of the proposed method is assessed by quantitative and qualitative measures.

This paper is organized as follows. Section 2 describes some important concepts and related work on super-resolution. Section 3 presents the proposed super-resolution method applied to a sequence of images. Experimental results are shown and discussed in Section 4. Finally, Section 5 concludes the paper with final remarks.

2 RELATED WORK

Spatial resolution is associated with the size of the smallest details visible in the image. The smaller the sampling interval among the image points, that is, the higher the density of points in the image, the higher the spatial resolution of the image. This does not mean that an image containing a large number of pixels necessarily has higher spatial resolution than one with fewer pixels.

Several super-resolution methods have been proposed in the literature for improving the spatial resolution of the images. The main objective of these methods is to estimate a high-resolution (HR) image from one or more low resolution (LR) images in order to highlight details, without the addition of artifacts in the resulting image.

The main approaches found in the literature can be classified into three categories: methods based on detail enhancement, reconstruction-based methods and learning-based methods. These approaches are described below.

2.1 Methods based on Detail Enhancement

In methods based on detail enhancement, the estimation of pixel values in the high resolution image is performed by interpolating the intensity or color of the pixels already present in the input image. Afterwards, a process is applied to reduce artifacts included in the interpolated images.

There are several interpolation methods in the literature (Gonzalez and Woods, 2007; Lucien et al., 1997), such that the most commonly used are the nearest neighbor, bilinear and bicubic interpolation.

In the nearest neighbor interpolation, the original pixel value $f(x,y)$ is assigned to the nearest pixel $f'(x',y')$ in the resampled image. Although the method is simple and has low computational cost, its main disadvantages are the generation of distortion in fine details and creation of jagged edges in the image.

The bilinear interpolation calculates the intensity of each pixel value $f'(x',y')$ by the weighted average of four pixels adjacent away from the nearest neighbors. The resulting image presents smoothing at the edges and phase distortion, resulting in image blurring.

Bicubic interpolation seeks to obtain a smooth estimate of the gray level or color at each pixel $f'(x,y)$ from a larger number of neighboring points of the original image, which form a polynomial of low degree. Fine details are preserved, edges are smoothed and distortions are minimized in the resulting image.

The super-resolution method called prior gradient profile (GPP) is a parametric distribution that describes the shape and sharpness of gradient profiles in natural images. One of the observations presented by Sun et al. (Sun et al., 2008; Sun et al., 2010) is that the statistical form of these profiles is stable and invariant to the resolution of the image. From this information, a statistical relation of the image gradient sharpness can be learned between HR and LR images.

Using the learned profile gradient relation, it is possible to provide a constraint on the field gradient of the HR image. Combining it with the constraint reconstruction, it is possible to recover a high quality image. The advantages of the GPP mentioned in (Sun et al., 2008; Sun et al., 2010) include: (a) the gradient profile is not a constraint of smoothness, therefore, the edges can be well recovered in the HR image both at small and large scales; (b) the artifacts common in super-resolution, such as jagged edges, can be avoided in the field gradient.

The high-resolution image in the GPP technique can be obtained from the following equation

$$\mathrm{HR}^{t+1} = \mathrm{HR}^{t} - \tau \frac{\partial \mathrm{E(HR)}}{\partial \mathrm{HR}} \qquad (1)$$

where $\frac{\partial \mathrm{E(HR)}}{\partial \mathrm{HR}} = ((\mathrm{HR} * G) \downarrow - \mathrm{LR}) \uparrow * G - \beta(\nabla^2 \mathrm{HR} - \nabla^2 \mathrm{HR}^T)$, $\nabla^2 \mathrm{HR}^T(x) = r(d(x, x_0))\nabla^2 \mathrm{LR}^u$, G represents the Gaussian filter, $*$ is the convolution operator, $\downarrow$ is the down-sampling operator, $\nabla^2 \mathrm{HR}^T$ represents the image field gradient of the HR image, $\nabla^2 \mathrm{LR}^u$ represents the field gradient of the LR image, and $\uparrow$ is the up-sampling operator. Term $\nabla^2 \mathrm{HR}^T$ transforms the observed field gradient into the target field gradient by mapping the shape and sharpness profile of the observed gradient.

2.2 Methods based on Reconstruction

Reconstruction-based methods consist in the synthesis of a single high resolution image from a sequence of low-resolution images (Borman and Stevenson, 1998). In these methods, it is assumed that the captured images of low resolution (LR) are very similar to each other. There are few details that set them apart, allowing the generation of new information to recover the image details in high resolution (HR) (Patti and Altunbasak, 2001).

These methods recover details of sequences and add them to the estimated high-resolution image. Usually, they have three different phases: i) registration of the images, ii) generation of the high-resolution grid, where their values are interpolated from the recorded images, iii) removal of noise (Park et al., 2003).

Irani and Peleg (Irani and Peleg, 1991) developed a technique called iterative back-projection (IBP), similar to the method of back-projection developed for reconstruction of tomographic images. Each low-resolution pixel is modeled as the projection of a given region in the high resolution image that will be estimated. The process starts with a first estimate of the high resolution to simulate the low-resolution images. Iteratively, information is added to this estimated image, from a new gradient image, based on the error between the simulated images and the observed images. This gradient image is the sum of all errors between the low resolution image and the high-resolution image estimated by the transformation process given by the motion estimation between the low-resolution images. The method uses an iterative procedure to minimize the error between the original data and the output of the model.

Projection onto convex sets (POCS) (Stark, 1988) uses the low resolution image to produce a new image through subpixel displacements in rows and columns. The displacement aims at minimizing the effects of aliasing and allowing the retrieval of new information for the high resolution image.

The POCS method seeks to solve the problem from a priori information described in the form of convex sets of constraints. The search for this solution consists of finding a value that belongs to the intersection of the sets. This is an iterative method, which produces, for a finite number of steps, intermediate solutions. The iteration ends when convergence occurs or the process is interrupted by a predetermined criterion.

Some improvements in reconstruction methods based on POCS were developed by Patti and Altunbasak (Patti and Altunbasak, 2001). First, the discretization of the model of continuous image formation is enhanced to allow the use of high-order interpolation methods. Second, the constraint sets are modified to reduce the number of edges present in the estimated high resolution image.

Reconstruction by super-resolution produces an image or a set of high resolution images from a set of low-resolution images. In the last two decades, several super-resolution methods have been proposed, some of them presented in (Borman and Stevenson, 1998; Farsiu et al., 2004a). These methods are often very sensitive to noise and to their data model, which limits their usefulness. In (Farsiu et al., 2004b), an alternative approach was proposed using minimization standards and robust regularization before dealing with different data models and noise.

2.3 Methods based on Learning

In super-resolution methods based on learning, the main objective is to estimate information, which is not present in the original low-resolution image, from a set of training samples.

The method proposed by Yu et al. (Yu et al., 2008) for super-resolution of face images uses projection onto convex sets (POCS) and residual compensation. First, the original high resolution image is estimated by POCS and then the residual compensation is performed. The high frequency information in the image is reconstructed from the learning between the two training data sets of corresponding low and high resolution residual images. The super-resolution image is generated from the sum between the initially estimated image and the image reconstructed by the weights of learned residuals. The method uses a machine learning algorithm called locally linear embedding (LLE) (Chang et al., 2004).

First, the method reconstructs the high resolution image initially estimated by POCS, similar to the original high resolution image. Afterwards, it estimates the residual compensation and the high frequency information is reconstructed by learning between the correspondence of sets of high and low resolution residual images. Assuming a set of N vectors of dimension D (Yu et al., 2008), then

$$x = [x_1, x_2, ..., x_i, ..., x_N] \tag{2}$$

For a new vector x_0, the Euclidean distance d_i between all other vectors x is calculated as

$$d_i = \sqrt{(x_0 - x_i)^T (x_0 - x_i)} \tag{3}$$

The K nearest neighbors of x_0 are defined by the Euclidean distance and, therefore, the best weights w to rebuild x_0 from K neighbors are determined ($w = [w_1, w_2, ..., w_i, ..., w_N]$), where w_i represents the contribution of x_i for x_0 reconstruction. If x_i is not between the K nearest neighbors of x_0, then $w_i = 0$, else $0 < w_i < 1$ and $\sum_i w_i = 1$.

The optimal weight w_i is estimated using the least squares algorithm

$$w_i = \frac{\sum_j P_{i,j}}{\sum_i \sum_j P_{i,j}} \tag{4}$$

where $P = G^{-1}$ and G is the covariance matrix defined as

$$G_{i,j} = (x_0 - x_i)^T (x_0 - x_i) \tag{5}$$

Since G is a singular matrix, that is, it has no inverse, the optimal solution can not be found by Equation 5. A relatively simple solution is to assign a small value of α to the diagonal of G

$$G = G + \alpha \times I \tag{6}$$

where I is a unit matrix.

The learning method proposed in (Yu et al., 2008) considers an initial low resolution image g obtained by degrading f ($g = Hf$) and an initial estimate of super-resolution $\hat{f}$ obtained by the POCS method. From the known degrading model H, the low resolution residual is calculated as

$$\hat{g} = H\hat{f}r = g - \hat{g} \tag{7}$$

Using the LLE algorithm to learn the weights of the reconstruction from the low-resolution residual r and the set of residual images, the method reconstructs the high-resolution residual $\hat{s}$ from the calculated weights and the corresponding data at high resolution. From the high-resolution residual, super-resolution image $\hat{f_{n+1}}$ is obtained by

$$\hat{f_{n+1}} = \hat{f}_n + \alpha\hat{s} \in (0, 1] \tag{8}$$

3 PROPOSED METHOD

According to the previous section, there are three main approaches to enhancing image resolutions: methods based on detail enhancement, reconstruction-based methods and learning-based methods. The method proposed in this work is based on learning, in which training samples are used to estimate the information regarding details that are not present in the lower resolution images. This super-resolution technique has been inspired by (Yu et al., 2008), which employs residual compensation.

The method developed in this work considers a sequence of low resolution images that will be combined into a single higher resolution image.

The training set, which is sampled from the sequence being processed due to high similarity among the samples, needs to be pre-processed prior to the execution, as shown in Figure 2.

Image samples in the training set are considered as to be the high resolution (HR). These images will be smoothed and downsampled to obtain low resolution (LR) images. The LR images have their resolution increased, generating images called SR, which will be smoothed and downsampled to generate the images LR$'$. The low resolution residuals are estimated by the difference between LR and LR$'$, which the corresponding high resolution residuals are estimated by the difference between images HR and SR. Feature extraction is performed for each low resolution residuals, resulting on a feature vector.

After the pre-processing, the proposed super-resolution method for multiple images is executed, according to the steps shown in Figure 3. This process is described in the following paragraphs.

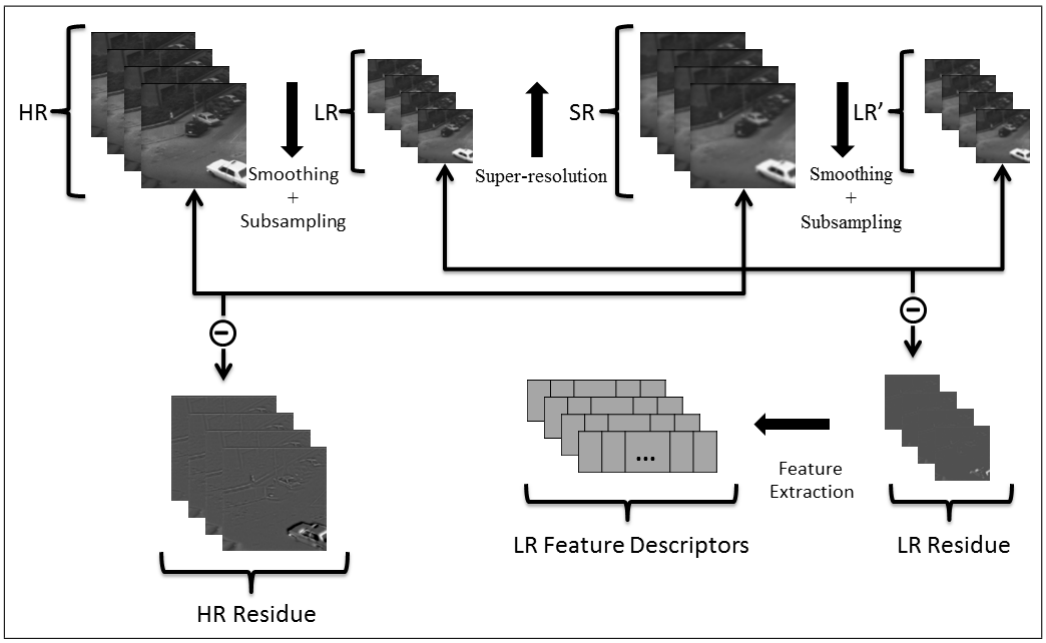

Figure 2: Pre-processing of the training set sampled from the image sequence.

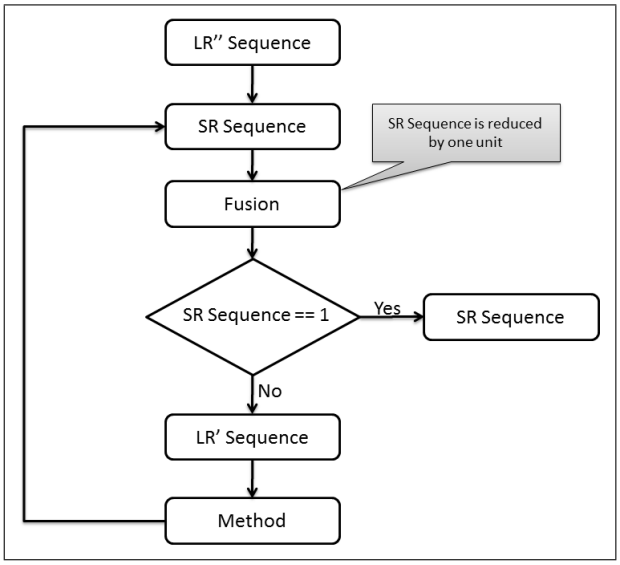

Figure 3: Data flow of the proposed method.

The execution process starts with the original sequence, denoted HR. This sequence is smoothed and then downsampled, which will generate a new sequence called LR. The proposed method will be applied to this sequence. This is necessary so that the original sequence can be used as a reference to assess the results achieved.

The second step consists of increasing the resolution of the sequence LR, generating a new sequence, called SR, with the same resolution as the original sequence. Then, the images are fused in pairs, in which one of them is the first images of the sequence (reference image), as shown in Figure 4.

The process starts with N images. After the fusion, the result consists of $N = N - 1$ images. If the sequence size N becomes equal to 1, the resulting super-resolved image has been obtained and the process is stopped. Otherwise, the resulting sequence is smoothed and downsampled, generating a new sequence LR$'$, in which the super-resolution for each image will be obtained by applying the procedure described in Section 3.1. This fusion process is illus-

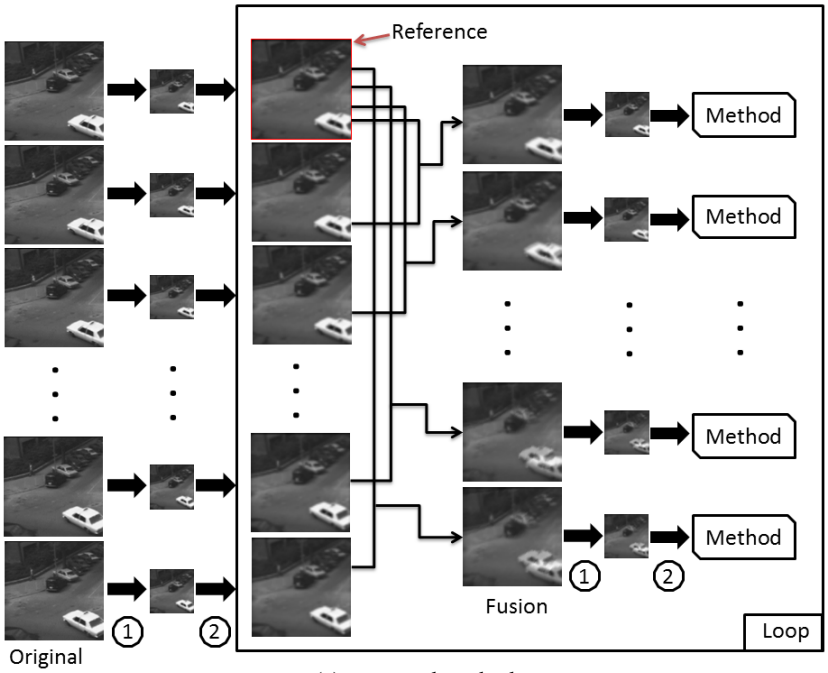

(a) proposed method

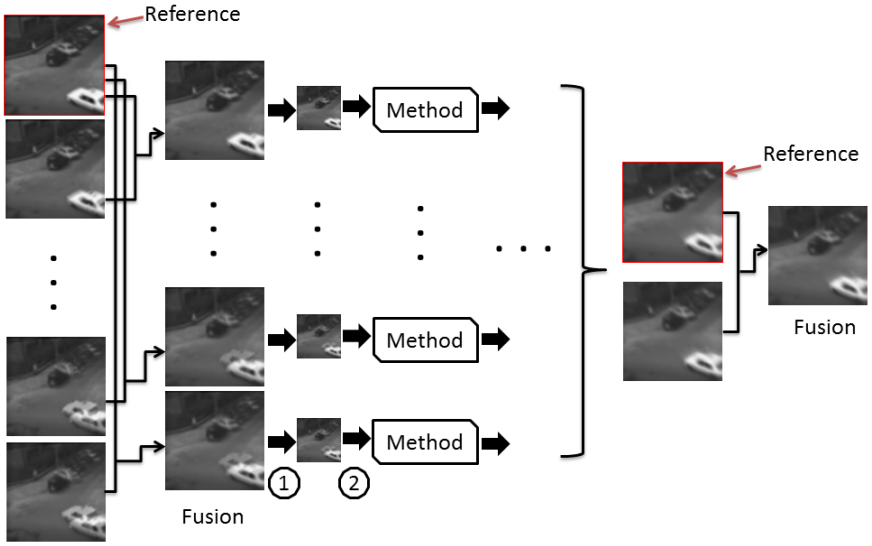

(b) iterative process

Figure 4: Proposed super-resolution method for a sequence of images.

trated in Figure 4(b) and Algorithm 1 presents the main steps of the method described during this section.

3.1 Super-Resolution for Single Images

The procedure to perform super-resolution for a single image is depicted in Figure 5. It starts by resampling the low resolution image (LR) to the desired size using a standard interpolation method such as bicubic, bilinear or nearest-neighbor, or another super-resolution method from the literature, such as GPP, POCS or IBP (described in Section 2). This results in an initial estimation of the super-resolved image, denoted SR.

If the initial estimation SR satisfies a similarity threshold based on the root mean square error (RMSE) between the LR and a smoothed and down-

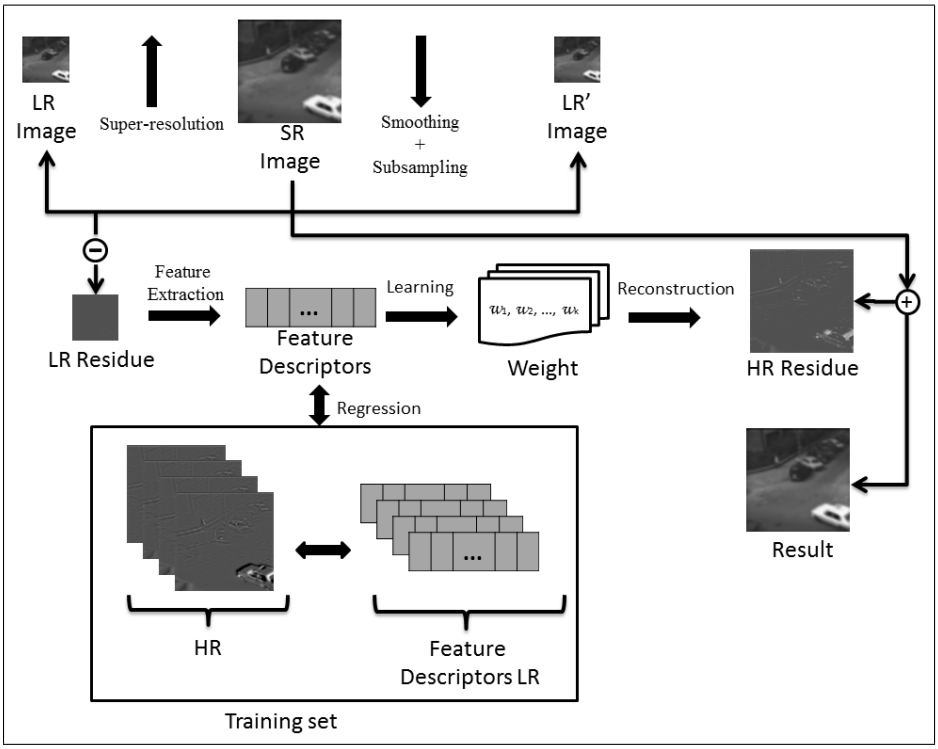

Figure 5: Super-resolution for single images.

Require: *img*: original image sequence, *n*: number of images on this sequence, *zoom*: zoom factor.
Ensure: *listSR*: resulting image.

1: **for all** $i = 2$ to n **do**
2: listImg$_{i-1}$ = fusion(downsample(img$_1$, *zoom*), downsample(img$_i$,*zoom*))
3: **end for**
4: $n \leftarrow n-1$
5: **while** $n > 1$ **do**
6: **for all** $i = 1$ to num_elements(listImg) **do**
7: test = smooth(listImg$_i$)
8: test = downsample(teste, 1/*zoom*)
9: listSR$_i$ = singleImage(test)
10: **end for**
11: **for all** $i = 2$ to n **do**
12: listAux$_{i-1}$ = fusion(listSR$_1$, listSR$_i$)
13: **end for**
14: listImg = listAux
15: $n \leftarrow n-1$
16: **end while**
17: **return** listSR

Algorithm 1: Image sequence super-resolution method.

sampled version of SR, the procedure stops. Otherwise, the image is modified by considering the residual information. SR is added to the high resolution residual according to Equation 9. This residual is reconstructed by the weighted sum of several samples belonging to the training set.

$$\mathrm{SR}_{n+1} = \mathrm{SR}_n + \alpha\,\mathrm{resHR} \tag{9}$$

To estimate the weights for the sum, features are extracted from the low resolution residuals (*resLR*) and added to a feature vector. From this vector, the weights of k nearest-neighbors are estimated using LLE (the k-th training samples which have the most similar residuals to *resLR*). Since feature vector is associated to a low and a high-resolution sample, the high resolution weights are used to estimate resHR in Equation 9, where $\alpha \in (0,1]$ denotes the importance of the residual estimation (this parameter is experimentally estimated in the next section). This process is repeated a certain number of iterations (also estimated experimentally in the next section).

4 EXPERIMENTAL RESULTS

This section describes the experiments and compares the results achieved by applying the proposed method. All experiments were conducted using a Intel Core 2 Duo 2.2 GHz processor with 6GBytes of RAM on the Windows 7 operating system.

Figure 6: Examples of frames for *taxi* video sequence (Nagel, 2011).

4.1 Dataset

To evaluate the proposed method, a public access video sequence with 41 frames was used (Nagel, 2011) (some frames are shown in Figure 6). Each frame is in grayscale and has 256×191 pixels. In our experiments, the frames were cropped to 128×128 pixels, since some of the compared methods work only for square images.

4.2 Evaluation Metrics

The results obtained were assessed through the root mean square error (RMSE) and the structural similarity (SSIM), quantitative and qualitative measures, respectively.

RMSE considers two images of equal sizes, such that RMSE equal to 0 represents that both images are identical. In the experiments, we consider the difference between the reference image and the resulting super-resolved image. Equation 10 shows the RMSE, where M and N denote the image dimensions.

$$\mathrm{RMSE} = \sqrt{\frac{1}{MN}\sum_{x=0}^{M-1}\sum_{y=0}^{N-1}[\mathrm{SR}(x,y) - \mathrm{HR}(x,y)]^2} \tag{10}$$

SSIM, proposed in (Wang et al., 2004), measures the similarity between two images considering local correlation, contrast and structures according to

$$\mathrm{SSIM}(x,y) = \frac{(2\mu_x\mu_y + C_1)(2\sigma xy + C_2)}{(\mu_x^2 + \mu_y^2 + C_1)(\sigma_x^2\sigma_y^2 + C_2)} \tag{11}$$

where constants C_1 and C_2 prevent from numerical instabilities when $(\mu_x^2 + \mu_y^2)$ and $(\sigma_x^2\sigma_y^2)$ are close to zero. As suggested in (Wang et al., 2004), we used $C_1 = 0.01$ and $C_2 = 0.03$. In this measure, the resulting values are normalized between 0 and 1, and the closer to 1, the better the image quality.

4.3 Parameter Settings

To evaluate the proposed method, a set of parameters has been defined in the experiments. First, the super-resolution method used to resample the input image to the desired size (as described in Section 3.1) was the GPP.

In the fusion process, the images are considered in pairs, in which one is considered as the reference image. As illustrated in Figure 4(b), the reference image corresponds to the first image of the sequence. To fuse two images (lines 2 and 12 of Algorithm 1), the SIFT algorithm (Lowe, 2004) was applied to detect corresponding points (Figure 7). From such corresponding points an affine transform is computed to register both images.

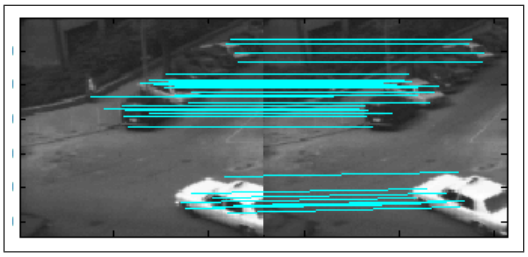

Figure 7: Corresponding points between two images used to fuse both images.

Finally, to achieve better results, experiments were conducted using different setups for parameters α (Equation 9) and the number of iterations for the super-resolution considering single images. According to Figure 8, the method presents higher accuracy for low values of α, such as 0.001. In addition to that, the best results have been achieved with 150 iterations.

4.4 Results and Comparisons

Using the parameters estimated in the previous section, the proposed method was compared to two video-based super-resolution methods: IBP (Irani and Peleg, 1991) and POCS (Stark, 1988) . Tables 1 and 2 show the results for zoom factors of 2× and 4× for image sequences with 6 and 12 frames (usually, long sequences are not considered due to the large amount of noise inserted). These values were achieved comparing the super-resolved image to the reference image (first image of the sequence).

Quantitative (Tables 1 and 2) and qualitative (Figure 9) results demonstrate the high accuracy of the proposed method. According to the results shown in Figure 9, it is also possible to see that the proposed

Table 1: Results achieved by the video-based super-resolution methods for a zoom factor of 2×.

Zoom factor 2×				
Method	6 frames		12 frames	
	RMSE	SSIM	RMSE	SSIM
IBP (Irani and Peleg, 1991)	32.5863	0.7476	34.0467	0.7081
POCS (Stark, 1988)	22.4413	0.8511	30.0020	0.7442
Proposed	**10.7686**	**0.9604**	**18.0773**	**0.8893**

Table 2: Results achieved by the video-based super-resolution methods for a zoom factor of 4×.

Zoom factor 4×				
Method	6 frames		12 frames	
	RMSE	SSIM	RMSE	SSIM
IBP (Irani and Peleg, 1991)	29.8295	0.7648	30.7796	0.7417
POCS (Stark, 1988)	21.5620	0.8571	29.4161	0.7501
Proposed	**14.0965**	**0.9303**	**16.1489**	**0.9161**

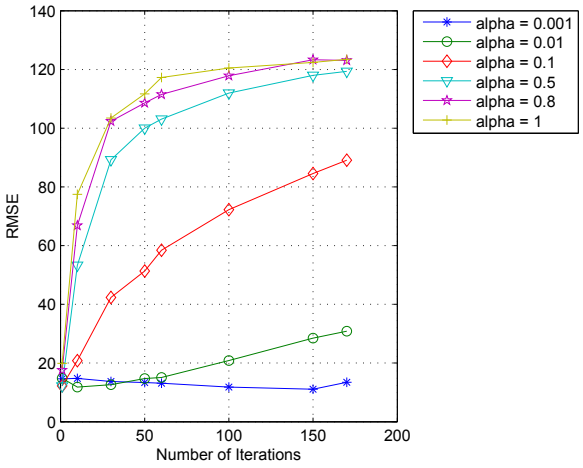

Figure 8: RMSE as a function of the number of iterations and α.

method presents sharper super-resolved images compared to the other methods.

5 CONCLUSIONS

Due to the increasing demand for high resolution images and sensor limitations, super-resolution techniques are fundamental tools to obtain high resolution data.

This work proposed a super-resolution technique based on the fusion of multiple images through residual compensation using a learning technique and feature extraction. The comparisons performed in our experiments showed that the proposed method achieved higher accuracy when compared to other approaches available in the literature.

ACKNOWLEDGMENTS

The authors are grateful to FAPESP, CAPES and CNPq for the financial support. This research was partially supported by FAPESP grant 2010/10618-3.

REFERENCES

Baker, S. and Kanade, T. (2002). Limits on Super-Resolution and How to Break Them. *IEEE Transactions on Pattern Analysis and Machine Intelligence*, 24(9):1167–1183.

Bascle, B., Blake, A., and Zisserman, A. (1996). Motion Deblurring and Super-resolution from an Image Sequence. In *Fourth European Conference on Computer Vision*, pages 573–582. Springer-Verlag.

Borman, S. and Stevenson, R. L. (1998). Super-Resolution from Image Sequences - A Review. In *Midwest Symposium on Circuits and Systems*, pages 374–378.

Chang, H., Yeung, D.-Y., and Xiong, Y. (2004). Super-Resolution through Neighbor Embedding. In *IEEE Conference on Computer Vision and Pattern Recognition (CVPR)*, pages 275–282.

Chaudhuri, S. (2001a). *Super-Resolution Imaging*. The Springer International Series in Engineering and Computer Science.

Chaudhuri, S. (2001b). *Super-Resolution Imaging*. Kluwer Academic Publishers.

Farsiu, S., Robinson, D., Elad, M., and Milanfar, P. (2004a). Advances and Challenges in Super-Resolution. *International Journal of Imaging Systems and Technology*, 14:47–57.

Farsiu, S., Robinson, M. D., Elad, M., and Milanfar, P. (2004b). Fast and Robust Multiframe Super Resolution. *IEEE Transactions on Image Processing*, 13(10):1327–1344.

Gonzalez, R. and Woods, R. (2007). *Digital Image Processing*. Prentice Hall.

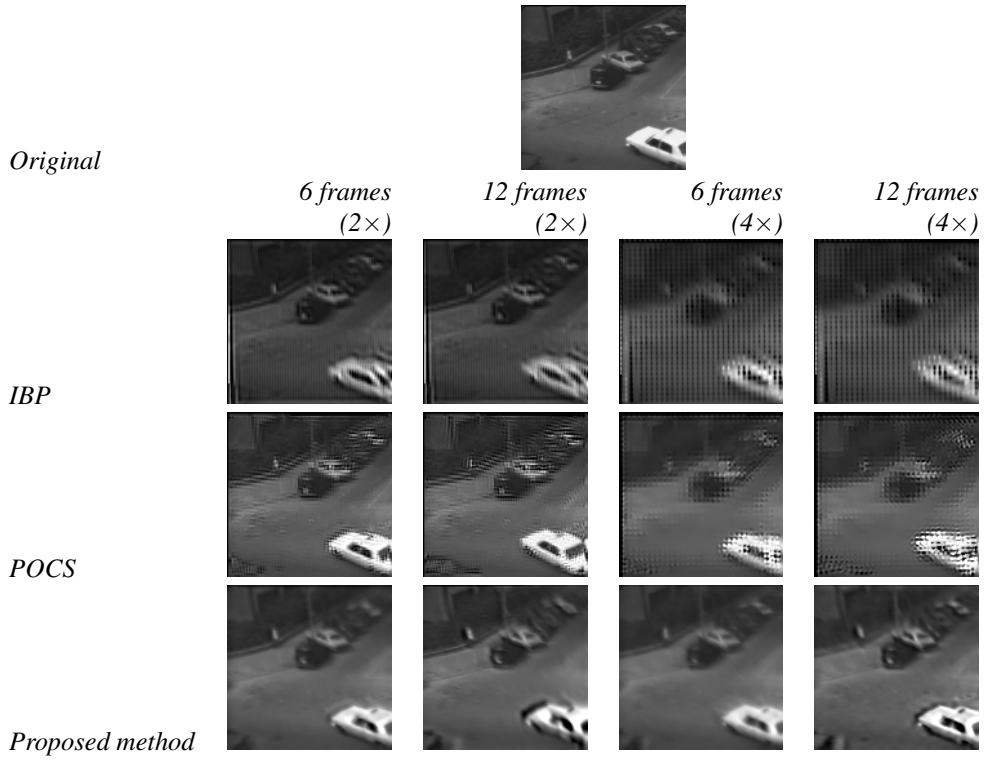

Figure 9: Results obtained for zoom factors of 2× and 4× and for sequences with 6 and 12 frames.

Irani, M. and Peleg, S. (1991). Improving Resolution by Image Registration. *Graphical Models and Image Processing*, 53(3):231–239.

Lin, F. C., Fookes, C. B., Chandran, V., and Sridharan, S. (2005). Investigation into Optical Flow Super-Resolution for Surveillance Applications. In *APRS Workshop on Digital Image Computing: Pattern Recognition and Imaging for Medical Applications*, Brisbane, Australia.

Liu, X., Song, D., Dong, C., and Li, H. (2008). MAP-Based Image Super-Resolution Reconstruction. In *Proceedings of World Academy of Science*, pages 208–211.

Lowe, D. (2004). Distinctive Image Features from Scale-Invariant Keypoints. *International Journal of Computer Vision*, 60:91–110.

Lucien, W. (1999). Definitions and Terms of Reference in Data Fusion. *IEEE Transactions on Geosciences and Remote Sensing*, 37(3):1190–1193.

Lucien, W., Ranchin, T., and Mangolini, M. (1997). Fusion of Satellite Images of Different Spatial Resolutions: Assessing the Quality of Resulting Images. *Photogrammetric Engineering & Remote Sensing*, 63:691–699.

Nagel, H.-H. (2011). Image Sequence Server. Institut für Algorithmen und Kognitive Systeme, Universität Karlsruhe. `http://i21www.ira.uka.de/image_sequences/`.

Park, S. C., Park, M. K., and Kang, M. G. (2003). Super-Resolution Image Reconstruction: A Technical Overview. *IEEE Signal Processing Magazine*, 20(3):21–36.

Patti, A. J. and Altunbasak, Y. (2001). Artifact Reduction for Set Theoretic Super Resolution Image Reconstruction with Edge Adaptive Constraints and Higher-Order Interpolants. *IEEE Transactions on Image Processing*, 10(1):179–186.

Schwartz, W., da Silva, R., Davis, L., and Pedrini, H. (2011). A Novel Feature Descriptor Based on the Shearlet Transform. In *IEEE International Conference on Image Processing*, Brussels, Belgium.

Stark, H. (1988). Theory of Convex Projection and its Application to Image Restoration. *IEEE International Symposium on Circuits and Systems*, pages 963–964.

Sun, J., Sun, J., Xu, Z., and Shum, H.-Y. (2008). Image Super-resolution using gradient profile prior. *IEEE Conference on Computer Vision and Pattern Recognition*.

Sun, J., Sun, J., Xu, Z., and Shum, H.-Y. (2010). Gradient Profile Prior and Its Applications in Image Super-Resolution and Enhancement. *IEEE Transactions on Image Processing*.

Wang, Z., Bovik, A., Sheikh, H., and Simoncelli, E. (2004). Image Quality Assessment: From Error Visibility to Structural Similarity. *IEEE Transactions on Image Processing*, 13(4):600–612.

Yu, H., Xiang, M., Hua, H., and Chun, Q. (2008). Face Image Super-Resolution through POCS and Residue Compensation. *IET Conference Publications*, pages 494–497.